

Universality classes in two-component driven diffusive systems

V. Popkov^(1,2), J. Schmidt⁽¹⁾

⁽¹⁾*Institut für Theoretische Physik, Universität zu Köln,
Zùlpicher Str. 77, 50937 Cologne, Germany. and*

⁽²⁾*CSDC Università di Firenze, via G.Sansone 1, 50019 Sesto Fiorentino, Italy*

G.M. Schütz^(3,4)

⁽³⁾*Institute of Complex Systems II, Theoretical Soft Matter and Biophysics,
Forschungszentrum Jùlich, 52425 Jùlich, Germany and*

⁽⁴⁾*Interdisziplinàres Zentrum für Komplexe Systeme,
Universität Bonn, Brùhler Str. 7, 53119 Bonn, Germany*

(Dated: July 17, 2018)

We study time-dependent density fluctuations in the stationary state of driven diffusive systems with two conserved densities ρ_λ . Using Monte-Carlo simulations of two coupled single-lane asymmetric simple exclusion processes we present numerical evidence for universality classes with dynamical exponents $z = (1 + \sqrt{5})/2$ and $z = 3/2$ (but different from the Kardar-Parisi-Zhang (KPZ) universality class), which have not been reported yet for driven diffusive systems. The numerical asymmetry of the dynamical structure functions converges slowly for some of the non-KPZ superdiffusive modes for which mode coupling theory predicts maximally asymmetric z -stable Lévy scaling functions. We show that all universality classes predicted by mode coupling theory for two conservation laws are generic: They occur in two-component systems with nonlinearities in the associated currents already of the minimal order $\rho_\lambda^2 \rho_\mu$. The macroscopic stationary current-density relation and the compressibility matrix determine completely all permissible universality classes through the mode coupling coefficients which we compute explicitly for general two-component systems.

PACS numbers: 05.60.Cd, 05.20.Jj, 05.70.Ln, 47.10.-g

Keywords: Driven diffusive systems; Dynamical critical phenomena; Kardar-Parisi-Zhang equation; Nonlinear fluctuating hydrodynamics; Mode coupling theory

I. INTRODUCTION

Anomalous transport is the hallmark of many one-dimensional non-equilibrium systems even when interactions are short-ranged [1]. A common way of characterizing 1-d systems that exhibit anomalous transport is through the dynamical structure function which describes the time-dependent fluctuations of the long-lived modes in the stationary state. In systems with short-range interactions and one global conservation law (giving rise to one long-lived mode) only two universality classes are known to exist, the Gaussian universality class with dynamical exponent $z = 2$ (also describing diffusive fluctuations in equilibrium stationary states), and the superdiffusive Kardar-Parisi-Zhang (KPZ) universality class with dynamical exponent $z = 3/2$ [2] for systems driven out of equilibrium. The exact scaling form of the KPZ structure function was found some 10 years ago by Prähofer and Spohn for the polynuclear growth model [3] and for a driven diffusive system, viz. the asymmetric simple exclusion process [4]. Since then the scaling function, which is expected to be universal, has also been observed in various experiments [5, 6].

Superdiffusive fluctuations in systems with more than one conservation law are less well-studied. Stochastic dynamics have been considered for driven diffusive systems with two conservation laws. Naively one might expect both modes to be in the KPZ universality class. This guess is indeed confirmed for the Arndt-Heinzel-Rittenberg model [7] by using exact results for the steady state combined by fluctuating hydrodynamics and mode coupling theory [8] and also for a general class of multi-component exclusion processes [9]. It was also known for some time that one mode can be KPZ, while the other is diffusive, see [10] where exact microscopic and hydrodynamic limit arguments are used, and numerical work [11, 12] for related results.

Recently van Beijeren [13] studied a system with Hamiltonian dynamics with three conservation laws. He predicted KPZ-universality for the two sound modes of the system and a novel superdiffusive universality class with dynamical exponent $z = 5/3$ for the heat mode. The occurrence of a $5/3$ mode was subsequently demonstrated for FPU-chains [14, 15] with three conservation laws and generally for anharmonic chains [16] and a family of exclusion process with two conservation laws [17]. Also recent mathematically rigorous work indicates non-trivial anomalous behaviour fluctuations in systems with two conservation laws [18].

Stochastic interacting particle systems with two conservation laws exhibit extremely rich

behaviour in one dimension, including spontaneous symmetry breaking [7, 19–23] or phase separation [7, 20, 24–27] in nonequilibrium stationary states, see [28] for a review. Studying the coarse-grained time evolution of two-component systems with an umbilic point one finds shocks with unusual properties [29, 30]. It is the purpose of this paper to go beyond stationary and time-dependent mean properties and consider time-dependent fluctuations. Specifically, we show that the complete list of dynamical universality classes that, according to mode coupling theory, can appear in the presence of two conservation laws can be realized in driven diffusive systems with two conserved densities. To this end we compute the exact mode coupling matrices for general strictly hyperbolic two-component systems with the stationary current-density relation and stationary compressibility matrix as the only input. With these input data the scaling form of the dynamical structure function is completely determined, except in the presence of a diffusive mode where the phenomenological diffusion coefficient enters the scale factors in the scaling functions. With these results we use mode coupling theory for computing explicitly the scaling form of the dynamical structure function for two superdiffusive modes which have been not reported yet in the literature on driven diffusive systems. We also present simulation data for a family of exclusion processes which confirm the theoretical predictions.

This paper is organized in the following way. We first introduce the lattice model that we are going to study numerically (Section II). This is an extended version of the two-lane exclusion process presented in our earlier work [17] that allows us to relax constraints on the physically accessible parameter manifold. In Section III we first present some predictions of mode coupling theory and then use the theory to make predictions for our model. The numerical tests of these predictions and some mode coupling computations are presented in Section IV. We finish with some conclusions in Section V. In the appendix we perform the full computation of the mode coupling matrices for arbitrary strictly hyperbolic two-component systems.

II. TWO-LANE ASYMMETRIC SIMPLE EXCLUSION PROCESS

We consider a two-lane asymmetric simple exclusion process where particles hop randomly on two parallel chains with L sites each and periodic boundary conditions. Particles do not change lanes and they obey the hard core exclusion principle which forbids occupancy of a

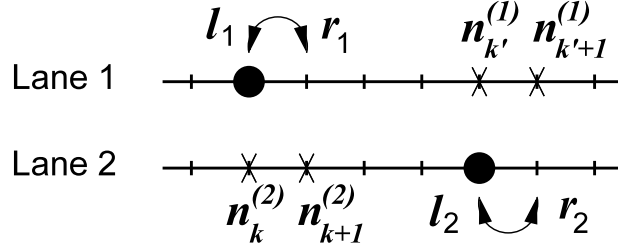


FIG. 1: Schematic representation of the two-lane partially asymmetric simple exclusion process. A particle on lane 1 (2) hops to the neighbouring site (provided this target site is empty) with to the right or left with rates (1) that depend on the particle configuration on the adjacent sites of the other lane that are marked by a cross.

site by more than one particle. We denote the particle occupation number on site k in the first (upper) lane by $n_k^{(1)} \in \{0, 1\}$, and on the second (lower) lane by $n_k^{(2)} \in \{0, 1\}$. The total particle number is conserved in each lane and denoted N_λ .

A hopping event from site k to site $k + 1$ on the same lane may happen if site k is occupied and site $k + 1$ on the same lane is empty. The rate of hopping depends on the particle configuration on the adjacent lane as follows: Particles on lane λ hop from site k to site $k + 1$ with rate $r_\lambda(k, k + 1)$ and from site $k + 1$ to site k with rate $\ell_\lambda(k + 1, k)$ (Fig. 1). The rates are given by

$$\begin{aligned}
 r_1(k, k + 1) &= p_1 + b_1 n_k^{(2)} + c_1 n_{k+1}^{(2)} + d_1 n_k^{(2)} n_{k+1}^{(2)} \\
 \ell_1(k + 1, k) &= q_1 + e_1 n_k^{(2)} + f_1 n_{k+1}^{(2)} + g_1 n_k^{(2)} n_{k+1}^{(2)} \\
 r_2(k, k + 1) &= p_2 + b_2 n_k^{(1)} + c_2 n_{k+1}^{(1)} + d_2 n_k^{(1)} n_{k+1}^{(1)} \\
 \ell_2(k + 1, k) &= q_2 + e_2 n_k^{(1)} + f_2 n_{k+1}^{(1)} + g_2 n_k^{(1)} n_{k+1}^{(1)}.
 \end{aligned} \tag{1}$$

The hopping attempts of particles from site k on lane λ to neighbouring sites occur independently of each other, after an exponentially distributed random time with mean $\tau_\lambda(k) = [r_\lambda(k, k + 1) + \ell_\lambda(k, k - 1)]^{-1}$ for a jump from site k on lane λ . Hopping attempts on an already occupied site are rejected.

Using pairwise balance [31] it is easy to verify that for any pair of total particle numbers N_λ the stationary distribution for this model is the uniform distribution, provided that the symmetry constraints $b_1 - e_1 = c_2 - f_2$, $b_2 - e_2 = c_1 - f_1$, $d_1 = g_1$ and $d_2 = g_2$ are met for the interaction constants between the two lanes. The “bare” hopping rates p_1, p_2, q_1, q_2 are arbitrary. From the canonical uniform measures one constructs stationary grandcanonical

product measures where each site of lane λ is occupied independently of the other sites with probability $\rho_\lambda \in [0, 1] = N_\lambda/L$. Hence the ρ_λ are the conserved densities of the grandcanonical stationary distribution, which, by construction, is the convex combination of all uniform measures with weight $[\rho_1/(1 - \rho_1)]^{N_1}[\rho_2/(1 - \rho_2)]^{N_2}$ and $0 \leq N_\lambda \leq L$.

From the hopping rates (1) and the product form of the grandcanonical distribution one reads off the corresponding stationary current vector \vec{j} with components

$$\begin{aligned} j_1(\rho_1, \rho_2) &= \rho_1(1 - \rho_1)(a + \gamma\rho_2), \\ j_2(\rho_1, \rho_2) &= \rho_2(1 - \rho_2)(b + \gamma\rho_1). \end{aligned} \quad (2)$$

with

$$a = p_1 - q_1, \quad b = p_2 - q_2, \quad \gamma = b_1 + c_1 - e_1 - f_1. \quad (3)$$

Notice that this current-density relation depends on the microscopic details of the model only through the parameter combinations a, b, γ which can take arbitrary real values. For $b = 1$ we recover the totally asymmetric two-lane model of [32] which is a special case of the multi-lane model of [33]. Throughout this work we set $a = 1, \gamma \neq 0$.

The product measure corresponds to a grandcanonical ensemble with a fluctuating particle number. These fluctuations are described by the symmetric compressibility matrix K with matrix elements

$$K_{\lambda\mu} := \frac{1}{L} \langle (N_\lambda - \rho_\lambda L)(N_\mu - \rho_\mu L) \rangle = \rho_\lambda(1 - \rho_\lambda)\delta_{\lambda,\mu}. \quad (4)$$

where $\lambda, \mu \in \{1, 2\}$. In the notation defined in the appendix this corresponds to

$$\kappa_\lambda := K_{\lambda\lambda} = \rho_\lambda(1 - \rho_\lambda), \quad \bar{\kappa} := K_{12} = 0. \quad (5)$$

As discussed below the current density relation \vec{j} given in (2) and the compressibility matrix K given (4) are the input data which completely determine the scaling functions describing the large scale behaviour of the particle system, up to a scale factor if a diffusive mode is relevant.

For the Monte-Carlo simulations presented in this paper we consider the totally asymmetric version of the model [17] where $p_1 = 1, p_2 = b, q_\lambda = e_\lambda = f_\lambda = g_\lambda = d_\lambda = 0$ and $b_\lambda = c_\lambda = \gamma/2 \neq 0$ with $\gamma > -\min(1, b)$. Initially we put N_λ particles randomly drawn from the stationary distribution, i.e., they are placed uniformly on lane λ . For the dynamics we perform random sequential updates where a site k_λ is chosen uniformly and a particle, if present and allowed to jump, jumps with a normalized

probability given by (1). One Monte-Carlo time unit then corresponds to $2L$ consecutive update attempts. We compute the empirical dynamical structure function defined by $\bar{S}_k^{\lambda\mu}(t) = 1/n \sum_{j=1}^n 1/L \sum_{l=1}^L n_{l+k}^{(\lambda)}(j\tau + t)n_l^{(\mu)}(j\tau) - \rho_\lambda\rho_\mu$ where for numerical efficiency we exploit translation variance and take a sum over n multiples of τ and over m Monte-Carlo histories. Time t and system size L are chosen such that finite-size corrections to the stationary current (which are of order $1/L$) and to the structure function (at most of order $1/L^{1+\alpha}$ with $\alpha > 1$ as discussed below) are small in absolute terms and negligible compared to statistical errors.

III. DYNAMICAL UNIVERSALITY CLASSES

A. Fluctuating hydrodynamics and mode coupling theory

Following the ideas set out in [34, 35] the starting point for investigating the large-scale dynamics of a microscopic lattice model is the system of conservation laws

$$\frac{\partial}{\partial t}\vec{\rho}(x, t) + \frac{\partial}{\partial x}\vec{j}(x, t) = 0 \quad (6)$$

where component $\rho_\lambda(x, t)$ of the density vector $\vec{\rho}(x, t)$ is the coarse-grained local density of the component λ of the system, and the component $j_\lambda(x, t)$ of the current vector $\vec{j}(x, t)$ is the associated current. The current is a function of x and t only through its dependence on the local conserved densities. Hence these equations can be rewritten as

$$\frac{\partial}{\partial t}\vec{\rho}(x, t) + J\frac{\partial}{\partial x}\vec{\rho}(x, t) = 0 \quad (7)$$

where J is the current Jacobian with matrix elements $J_{\lambda\mu} = \partial j_\lambda / \partial \rho_\mu$. The product JK of the Jacobian with the compressibility matrix (4) is symmetric [36] which guarantees that the system (7) is hyperbolic [37]. The eigenvalues v_α of J are the characteristic velocities of the system. If $v_1 \neq v_2$ the system is called strictly hyperbolic. Notice that in our convention $\vec{\rho}$ and \vec{j} are regarded as column vectors. Transposition is denoted by a superscript T .

Eq. (7) describes the deterministic time evolution of the density under Eulerian scaling where the lattice spacing a is taken to zero such that $x = ka$ remains finite and at the same time the microscopic time τ is taken to infinity such that the macroscopic time $t = \tau a$ is finite. The effect of fluctuations, which occur on finer space-time scales where $t = \tau a^z$ with dynamical exponent $z > 1$, can be captured by adding phenomenological white noise terms

ξ_i and taking the non-linear fluctuating hydrodynamics approach together with a mode-coupling analysis of the non-linear equation. Following [16] we summarize here the main ingredients of this well-established description.

One expands the local densities $\rho_\lambda(x, t) = \rho_\lambda + u_\lambda(x, t)$ around their long-time stationary values ρ_λ and keeps terms to first non-linear order in the fluctuation fields $u_\lambda(x, t)$. For quadratic nonlinearities (7) then yields

$$\partial_t \vec{u} = -\partial_x \left(J\vec{u} + \frac{1}{2} \vec{u}^T \vec{H} \vec{u} - D \partial_x \vec{u} + B \vec{\xi} \right) \quad (8)$$

where \vec{H} is a column vector whose entries $(\vec{H})_\lambda = H^\lambda$ are the Hessians with matrix elements $H_{\mu\nu}^\lambda = \partial^2 j_\lambda / (\partial \rho_\mu \partial \rho_\nu)$. The term $\vec{u}^T H^\lambda \vec{u}$ denotes the inner product in component space. The diffusion matrix D is a phenomenological quantity. The noise strength B does not appear explicitly below, but plays an indirect role in the mode-coupling analysis. One recognizes in (8) a system of coupled noisy Burgers equations. If the quadratic non-linearity is absent one has diffusive behaviour, up to possible logarithmic corrections that may arise from cubic non-linearities [38].

In order to analyze this nonlinear equation we transform to normal modes $\vec{\phi} = R\vec{u}$ where $RJR^{-1} = \text{diag}(v_\alpha)$ and the transformation matrix R is normalized such that $RKR^T = \mathbf{1}$, see the appendix. From (8) one thus arrives at

$$\partial_t \phi_\alpha = -\partial_x \left(v_\alpha \phi_\alpha + \vec{\phi}^T G^\alpha \vec{\phi} - \partial_x (\tilde{D} \vec{\phi})_\alpha + (\tilde{B} \vec{\xi})_\alpha \right) \quad (9)$$

with $\tilde{D} = RDR^{-1}$, $\tilde{B} = RB$ and

$$G^\alpha = \frac{1}{2} \sum_\lambda R_{\alpha\lambda} (R^{-1})^T H^\lambda R^{-1} \quad (10)$$

are the mode coupling matrices.

To make contact of this macroscopic description with the microscopic model we first note that the current-density relation given by the components of the current vector \vec{j} arises from the microscopic model by computing the stationary current-density relations $j_\lambda(\rho_1, \rho_2)$ and then substituting the stationary conserved densities by the coarse-grained local densities $\rho_\lambda(x, t)$ which are regarded as slow variables. Similarly, the compressibility matrix K is computed from the stationary distribution. Hence the mode coupling matrices (and with them the dynamical universality classes as shown below) are completely determined by these two macroscopic stationary properties of the system. We stress that the *exact* stationary

current-density relations and the *exact* stationary compressibilities are required. Approximations obtained e.g. from stationary mean field theory will, in general, only accidentally provide the information necessary for determining the dynamical universality classes of the system. In the appendix we compute the mode coupling matrices of a general two-component system with the current vector and compressibility matrix as input parameters.

Second, consider the dynamical structure matrix $\bar{S}_k(t)$ of the microscopic model defined on the lattice.[42] Its matrix elements are the dynamical structure functions

$$\bar{S}_k^{\lambda\mu}(t) := \langle (n_k^{(\lambda)}(t) - \rho_\lambda)(n_0^{(\mu)}(t) - \rho_\mu) \rangle \quad (11)$$

which measure density fluctuations in the stationary state. This quantity has two different physical interpretations. On the one hand, one can regard the random variable $f_k^\lambda(t) := n_k^{(\lambda)}(t) - \rho_\lambda$ as a stochastic process and then the dynamical structure function describes the stationary two-time correlations of this process. The long-time behaviour of the dynamical structure function can thus be determined from the fluctuation fields $u_\lambda(x, t)$ appearing in the non-linear fluctuating hydrodynamics approach (8), i.e., $\bar{S}_k^{\lambda\mu}(t) \xrightarrow{k, t \rightarrow \infty} \langle u_\lambda(x, t)u_\mu(0, 0) \rangle$. In a different interpretation the dynamical structure function measures the time evolution of the expectation of $f_k^\lambda(t)$ at time t , i.e., the unnormalized density profiles $\bar{\rho}_k^\lambda(t) := \langle n_k^{(\lambda)}(t) - \rho_\lambda \rangle$ that at time $t = 0$ have a delta-peak at site 0. Since the two conserved quantities interact, an initial perturbation even of only one component will cause a non-trivial relaxation of *both* density profiles. In each component the initial peak will evolve into two separate peaks, which move and spread with time. The characteristic velocities v_α are the collective velocities, i.e., the center-of-mass velocities of the two local perturbations [32]. The variance of the evolving density profiles determines the collective diffusion coefficient. This second interpretation of the dynamical structure matrix as describing a relaxation process, completely equivalent to the first fluctuation interpretation, is quite natural from the viewpoint of regarding (8) as a more detailed description of (6) in the sense of describing fluctuation effects on finer space-time scales due to the randomness of the stochastic process from which (6) arises under Eulerian scaling.

Analogously one can regard the transformed modes of the lattice model $\vec{\phi}_k(t) = R\vec{f}_k(t)$ in the fluctuation interpretation as stationary processes and the transformed dynamical structure functions

$$S_k^{\alpha\beta}(t) = [R\bar{S}_k(t)R^T]_{\alpha\beta} = \langle \phi_k^\alpha(t)\phi_0^\beta(0) \rangle \quad (12)$$

as the stationary space-time fluctuations. The transformation of the dynamical structure functions to the normal modes $\vec{\phi}_k(t)$ on the lattice, which is important for the numerical simulation of lattice models, is discussed in more detail in Appendix A. The large-scale behaviour of $S_k^{\alpha\beta}(t)$ is given in terms of the normal modes $\phi_\alpha(x, t)$ appearing in (9) by $S_{\alpha\beta}(x, t) = \langle \phi_\alpha(x, t)\phi_\beta(0, 0) \rangle$. In the second relaxation interpretation the normal modes are seen as local perturbations of a stationary distribution with a specific choice of initial amplitudes in each component.

Since for strictly hyperbolic systems the two characteristic velocities are different, one expects that the off-diagonal elements of S decay quickly. For long times and large distances one is thus left with the diagonal elements which we denote by

$$S_\alpha(x, t) := S^{\alpha\alpha}(x, t) \quad (13)$$

with initial value $S_\alpha(x, 0) = \delta(x)$. The large scale behaviour of the diagonal elements is expected to have the scaling form

$$S_\alpha(x, t) \sim t^{-1/z_\alpha} f_\alpha((x - v_\alpha t)^{z_\alpha}/t) \quad (14)$$

with a dynamical exponent z_α that may be different for the two modes. The exponent in the power law prefactor follows from mass conservation. In momentum space one has

$$\hat{S}_\alpha(p, t) \sim e^{-iv_\alpha pt} \hat{f}_\alpha(p^{z_\alpha t}) \quad (15)$$

for the Fourier transform

$$\hat{S}_\alpha(p, t) := \frac{1}{\sqrt{2\pi}} \int_{-\infty}^{\infty} dx e^{-ipx} S_\alpha(x, t). \quad (16)$$

Whether the difference of the characteristic speeds vanishes or not plays an important role. For the case where $v_1 = v_2$, i.e., when the system (7) has an umbilic point, it was found numerically in the framework of dynamic roughening of directed lines that the dynamical exponent is $z = 3/2$, but the scaling functions are not KPZ [40]. On the other hand, for strictly hyperbolic systems the normal modes have different speeds and hence their interaction becomes very weak for long times. By identifying ϕ_α with the gradient of a height variable (9) then turns generically into two decoupled KPZ-equations with coefficients $G_{\alpha\alpha}^\alpha$ determining the strength of the nonlinearity.

In order to analyze the system of nonlinear stochastic PDE's in more detail we employ mode coupling theory [16]. The basic idea is to capture the combined effect of non-linearity

and noise by a memory kernel. Thus the starting point for computing the $S_\alpha(x, t)$ are the mode coupling equations

$$\partial_t S_\alpha(x, t) = (-v_\alpha \partial_x + D_\alpha \partial_x^2) S_\alpha(x, t) + \int_0^t ds \int_{-\infty}^{\infty} dy S_\alpha(x - y, t - s) \partial_y^2 M_{\alpha\alpha}(y, s) \quad (17)$$

with the diagonal element $D_\alpha := \tilde{D}_{\alpha\alpha}$ of the phenomenological diffusion matrix and the memory kernel

$$M_{\alpha\alpha}(y, s) = 2 \sum_{\beta, \gamma} (G_{\beta\gamma}^\alpha)^2 S_\beta(y, s) S_\gamma(y, s). \quad (18)$$

The strategy is to plug into this equation, or into its Fourier representation, the scaling ansatz (14) (or (15)). One gets equations for the dynamical exponents arising from requiring non-trivial scaling solutions and using the known results $z = 3/2$ for KPZ and $z = 2$ for diffusion. In a next step one can then solve for the actual scaling functions, see below. Since for $v_1 \neq v_2$ one has $S_\beta(y, s) S_\gamma(y, s) \approx 0$ for $\beta \neq \gamma$ it is clear that the scaling behaviour of the solutions of (17) will be determined largely by the diagonal terms $G_{\beta\beta}^\alpha$ of the mode coupling matrices G^α . If a leading self-coupling term $G_{\alpha\alpha}^\alpha$ vanishes, one finds non-KPZ behaviour for mode α . In particular, if all diagonal terms are zero, the mode is diffusive. A coupling of a diffusive mode to a KPZ-mode leads to a modified KPZ-mode [39]. Thus the crucial property of the mode coupling matrices is whether a diagonal element is zero or not.

Some algebra along the lines of [16] involving power counting then yields the complete list of possible universal classes of strictly hyperbolic two-component systems from the structure of the mode coupling matrices G^α as shown in Table I, see also [39] where a similar table was derived independently. The shorthand KPZ represents the KPZ scaling function, while KPZ' refers to modified KPZ, both with dynamical exponent $z = 3/2$. D represents a Gaussian scaling function f_α with dynamical exponent $z_\alpha = 2$, $z_\alpha L$ represents a z_α -stable Lévy distribution as scaling function f_α with dynamical exponent z_α , GM (for golden mean) represents φL with $\varphi = (1 + \sqrt{5})/2$. In what follows we apply these general results to the two-lane model defined above. It will transpire that all theoretically possible scenarios can actually be realized in this family of models.

B. Mode-coupling matrix for the two-lane model

The input data are the current-density relation (2) and the compressibility matrix (4). From the current-density relation one computes the current Jacobian and the Hessian, which

$\backslash G^1$	$\begin{pmatrix} \star \\ \bullet \end{pmatrix}$	$\begin{pmatrix} \star \\ 0 \end{pmatrix}$	$\begin{pmatrix} \mathbf{0} \\ \bullet \end{pmatrix}$	$\begin{pmatrix} \mathbf{0} \\ 0 \end{pmatrix}$
$G^2 \backslash$				
$\begin{pmatrix} \bullet \\ \star \end{pmatrix}$	(KPZ,KPZ)	(KPZ,KPZ)	$(\frac{5}{3}\text{L},\text{KPZ})$	(D,KPZ')
$\begin{pmatrix} 0 \\ \star \end{pmatrix}$	(KPZ,KPZ)	(KPZ,KPZ)	$(\frac{5}{3}\text{L},\text{KPZ})$	(D,KPZ)
$\begin{pmatrix} \bullet \\ \mathbf{0} \end{pmatrix}$	$(\text{KPZ},\frac{5}{3}\text{L})$	$(\text{KPZ},\frac{5}{3}\text{L})$	(GM,GM)	$(\text{D},\frac{3}{2}\text{L})$
$\begin{pmatrix} 0 \\ \mathbf{0} \end{pmatrix}$	(KPZ',D)	(KPZ,D)	$(\frac{3}{2}\text{L},\text{D})$	(D,D)

TABLE I: Classification of universal behaviour of the two modes by the structure of the mode coupling matrices G^α . The acronyms denote: KPZ: KPZ universality class (superdiffusive), KPZ': modified KPZ universality class (superdiffusive), D = Gaussian universality class (normal diffusion), $z_\alpha\text{L}$: superdiffusive universality class with z_α -stable Lévy scaling function and GM = φL with the golden mean $\varphi = (1 + \sqrt{5})/2$. An bullet or star in the G^α denotes a non-zero entry, no entry represents an arbitrary value (zero or non-zero). The selfcoupling terms $G_{\alpha\alpha}^\alpha$ are marked as star or boldface 0, resp.

are used together with the compressibility matrix to compute the basis for normal modes and finally the mode coupling matrices, as shown in detail in the appendix in the general case.

For the present model we remark first that the currents (2) are at most quadratic in each density. Hence no logarithmic corrections to diffusive behaviour are expected in the two-lane model defined above. Second, as discussed in the appendix, in any coupled two-component system a vanishing cross compressibility $\bar{\kappa} = 0$ (where $\lambda \neq \mu$) implies that the cross derivatives $\partial j_\lambda / \partial \rho_\mu$ of the currents have to be non-zero except when one of the two components is frozen, i.e., fully occupied or fully empty.

For our system the explicit form of J is

$$J = \begin{pmatrix} (1 + \gamma\rho_2)(1 - 2\rho_1) & \gamma\rho_1(1 - \rho_1) \\ \gamma\rho_2(1 - \rho_2) & (b + \gamma\rho_1)(1 - 2\rho_2) \end{pmatrix}. \quad (19)$$

and the Hessians H^λ are

$$H^1 = \begin{pmatrix} -2(1 + \gamma\rho_2) & \gamma(1 - 2\rho_1) \\ \gamma(1 - 2\rho_1) & 0 \end{pmatrix}, \quad H^2 = \begin{pmatrix} 0 & \gamma(1 - 2\rho_2) \\ \gamma(1 - 2\rho_2) & -2(b + \gamma\rho_1) \end{pmatrix}. \quad (20)$$

The parameters convenient for theoretical analysis are not the matrix elements of the current Jacobian and the Hessians, but the parameters u , $\omega = \tan \vartheta$ (A20) and the transformed Hessian parameters (A42), (A43) defined in the appendix to which we refer for the derivation of the following results. Here we point out only the relevant features of the quantities resulting from these lengthy but simple computations.

The collective velocities $v_{1,2}$ are given in (A4). Notice that $J_{12}J_{21} = \gamma^2\rho_1(1 - \rho_1)\rho_2(1 - \rho_2) \geq 0$ in the whole physical parameter regime of the model. In fact, unless one of the lanes is frozen we have the strict inequality $J_{12}J_{21} > 0$. The frozen case is of no interest since then the dynamics in the non-frozen lane reduce to the dynamics of a single exclusion process. Hence we shall assume $J_{12}J_{21} > 0$ throughout this paper. Therefore the discriminant of the characteristic polynomial of J (A3) is non-zero which implies that the model is strictly hyperbolic in the parameter domain of interest.

The transformation matrix R involves normalization factors z_{\pm} (A19) and the parameters u and $\omega = \tan \vartheta$ defined in (A20). From (19) we find

$$\omega = \frac{1 - b - (2 + b\gamma)\rho_1 + (\gamma + 2b)\rho_2}{2\gamma\sqrt{\rho_1(1 - \rho_1)\rho_2(1 - \rho_2)}} \left(1 + \sqrt{1 + \frac{4\gamma^2(\rho_1(1 - \rho_1)\rho_2(1 - \rho_2))}{(1 - b - (2 + b\gamma)\rho_1 + (\gamma + 2b)\rho_2)^2}} \right) \quad (21)$$

and

$$u = \sqrt{\frac{\rho_1(1 - \rho_1)}{\rho_2(1 - \rho_2)}}. \quad (22)$$

For $J_{11} = J_{22}$ one has $\omega = 1$.

From the Hessians (20) one obtains the mode coupling parameters (A42), (A43)

$$g_1^1 = -2(1 + \gamma\rho_2), \quad g_2^1 = 0, \quad \bar{g}^1 = \gamma\sqrt{\frac{\rho_2(1 - \rho_2)}{\rho_1(1 - \rho_1)}}(1 - 2\rho_1), \quad (23)$$

and

$$g_1^2 = 0, \quad g_2^2 = -2\sqrt{\frac{\rho_2(1 - \rho_2)}{\rho_1(1 - \rho_1)}}(b + \gamma\rho_1), \quad \bar{g}^2 = \gamma(1 - 2\rho_2). \quad (24)$$

The compressibility matrix enters the mode coupling coefficients only through the normalization factors z_{\pm} for which we obtain from (A25)

$$z_{\pm} = 1/\sqrt{\kappa_1} \notin \{0, \pm\infty\}. \quad (25)$$

This yields the desired diagonal elements of the mode coupling matrices

$$G_{\beta\beta}^{\alpha}(\omega) = A_0 D_{\beta}^{\alpha}(\omega) \quad (26)$$

with

$$D_1^1(\omega) = g_1^1 - 2\bar{g}^1\omega + 2\bar{g}^2\omega^2 - g_2^2\omega^3 \quad (27)$$

$$D_2^1(\omega) = (2\bar{g}^1 - g_2^2)\omega + (g_1^1 - 2\bar{g}^2)\omega^2 \quad (28)$$

$$D_1^2(\omega) = (g_1^1 - 2\bar{g}^2)\omega + (g_2^2 - 2\bar{g}^1)\omega^2 \quad (29)$$

$$D_2^2(\omega) = g_2^2 + 2\bar{g}^2\omega + 2\bar{g}^1\omega^2 + g_1^1\omega^3. \quad (30)$$

and

$$A_0 = \frac{1}{2}\sqrt{\kappa_1}\cos^3(\vartheta) \neq 0. \quad (31)$$

As discussed in the appendix the vanishing cross-compressibility $\bar{\kappa} = 0$ of our model guarantees that $A_0 \neq 0$. Therefore a diagonal element $G_{\beta\beta}^{\alpha}$ of a mode coupling matrix vanishes if and only if the polynomial D_{β}^{α} defined in (27) - (30) vanishes. In order to see whether all scenarios listed in Table I can be realized by making the appropriate diagonal matrix elements zero we study all these cases. The relation between vanishing diagonal elements and the universality class as well as the values of the dynamical exponents follows from straightforward power counting in the mode coupling equations derived in [16], see below for the two special cases we focus on in this work.

Purely diffusive case (D,D):

First consider the purely diffusive case (D,D) for which mode coupling theory requires $D_1^1 = D_2^1 = D_1^2 = D_2^2 = 0$. Demanding that $D_2^1 = D_1^2 = 0$ leads to the constraints $g_1^1 = 2\bar{g}^2$ and $g_2^2 = 2\bar{g}^1$. In terms of the parameters $b, \gamma, \rho_{\lambda}$ this reads $-\gamma = 1/(1 - \rho_2) = b/(1 - \rho_1)$. This is outside the physical parameter range $\gamma > -\min(1, b)$ of the totally asymmetric model of [17], but can be realized in the general two-lane model defined in Section II. Plugging this condition into $D_1^1 = D_2^2 = 0$ yields the further conditions that $g_1^1 = g_2^2 = 0$, i.e., both Hessians must vanish. This requires

$$\rho_1 = \rho_2 = 1/2, \quad b = 1, \quad \gamma = -2. \quad (32)$$

The characteristic velocities are then $v_{1,2} = \mp 1$. It is somewhat counterintuitive that for these values one has $j_1 = j_2 = 0$, i.e., the system appears to be macroscopically in equilibrium, but the Gaussian mass fluctuations travel with non-zero velocities. A simple parameter choice for this scenario is $p_1 = p_2 = 1$, $q_1 = d_1 = g_1 = q_2 = d_2 = g_2 = 0$, $b_1 = c_1 = b_2 = c_2 = -1/2$, $e_1 = f_1 = e_2 = f_2 = 1/2$.

Superdiffusive mixed cases (D,KPZ'), (D,KPZ), (D, $\frac{3}{2}$ L), (KPZ, $\frac{5}{3}$ L):

Consider $b = 1$ where the hopping rates are completely symmetric with respect to the lane interchange and take $\rho_1 = \rho_2 =: \rho$. Then $g_1^1 = g_2^2 = -2(1 + \gamma\rho)$, $g_2^1 = g_1^2 = 0$, $\bar{g}^1 = \bar{g}^2 = \gamma(1 - 2\rho)$ and $u = 1$, $\omega = 1$. This yields $D_1^1 = D_2^2 = 0$ and $D_2^1 = 2A_0(g_1^1 + 2\bar{g}^1)$, $D_1^2 = 2A_0(g_2^2 - 2\bar{g}^2)$ with $A_0 = \sqrt{\rho(1 - \rho)/32}$. Computing the off-diagonal elements from (A38), (A41) we find the full mode coupling matrices

$$G^1 = -4A_0(1 + \gamma\rho) \begin{pmatrix} 0 & 1 \\ 1 & 0 \end{pmatrix}, \quad G^2 = -4A_0 \begin{pmatrix} 1 + \gamma(1 - \rho) & 0 \\ 0 & 1 - \gamma(1 - 3\rho) \end{pmatrix} \quad (33)$$

Thus generically this line is in the (D,KPZ') universality class (Fig. 2).

Notice that at $\gamma = -1/(1 - \rho)$ one has $D_1^2 = 0$, corresponding to the (D,KPZ) universality class which can be realized in the generalized two-lane model defined above and that occurs also in the single-lane multi-component asymmetric simple exclusion process with stationary product measure [9]. For $\gamma = 1/(1 - 3\rho)$ one has $D_2^1 = 0$, corresponding to the (D, $\frac{3}{2}$ L) scenario, see next section. If one moves away from the line $\rho_1 = \rho_2$, but stays on the curves indicated in Fig. 2 for special values of γ the self-coupling coefficient G_{11}^1 is non-zero, but $G_{22}^2 = 0$. This can be straightforwardly verified by calculating the linear response of the diagonal elements of G^1, G^2 to small deviations $\delta\rho_1, \delta\rho_2$ from the line $\rho_1 = \rho_2$. Hence one has the (KPZ, $\frac{5}{3}$ L) scenario. The three cases (D,KPZ'), (D, $\frac{3}{2}$ L) and (KPZ, $\frac{5}{3}$ L) can be realized in the totally asymmetric two-lane model.

Golden mean universality class (GM,GM):

Next consider $b \neq 1$. The formulas for the mode coupling matrices become cumbersome and we do not present them here in explicit form in full generality. It turns out that one can

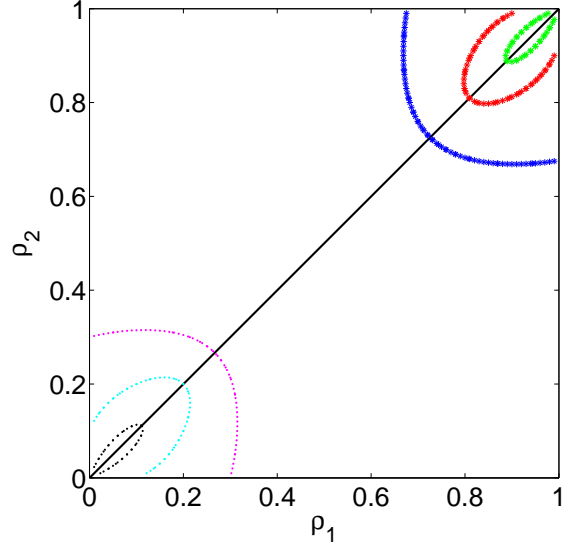


FIG. 2: (Colour online) Location of points where $G_{22}^2 = 0$, $G_{11}^2 \neq 0$ for $b = 1$ and different values of γ . In the upper right (lower left) corner the points grouped along curves of increasing length correspond to $\gamma = 1.5, 2.5, 5$ ($\gamma = -0.6, -0.7, -0.85$). On these curves one generically has the $(\frac{5}{3}\text{L}, \text{KPZ})$ universality class. On the diagonal line $\rho_1 = \rho_2$ one has $G_{11}^1 = G_{22}^1 = 0$, generically corresponding to the (D, KPZ') universality class. On the intersection of this line with a curve parametrized by γ one has the $(\text{D}, \frac{3}{2}\text{L})$ universality class.

have that both self-coupling coefficients $G_{\alpha\alpha}^\alpha$ vanish and both subleading diagonal elements $G_{\beta\beta}^\alpha$ with $\beta \neq \alpha$ are non-zero, corresponding to the $(\varphi\text{L}, \varphi\text{L})$ scenario where both dynamical exponents are the golden mean $\varphi = (1 + \sqrt{5})/2$, see Fig. 3. This can be realized by choosing unequal densities such that

$$(1 + \gamma\rho_2)(1 - 2\rho_1) = (b + \gamma\rho_1)(1 - 2\rho_2) \quad (34)$$

which corresponds to $J_{11} = J_{22}$ and hence $\omega = 1$. Then the requirement $D_1^1 = D_2^2 = 0$ yields

$$\rho_1 = \frac{1-b}{3\gamma}, \quad \rho_2 = \frac{\gamma-1}{3\gamma} \quad (35)$$

which implies $\gamma \in (-\infty, -1/2] \cup [1, \infty)$ and b is in the range between γ and -2γ . For general values of ω the analytical formulas for the lines $G_{11}^1 = G_{22}^2 = 0$ in the $\rho_1 - \rho_2$ plane are complicated. In order to demonstrate the existence of solutions we show numerical plots for fixed $\gamma = -3/4$ and various values b in Fig. 3. Notice also that there are parameter ranges of b without solutions in the physical range of densities $(\rho_1, \rho_2) \in [0, 1] \times [0, 1]$.

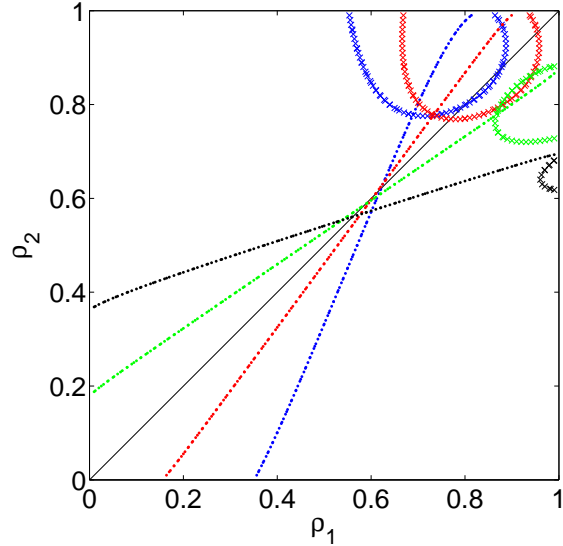


FIG. 3: (Colour online) Location of points where $G_{11}^1 = 0$ $G_{22}^1 \neq 0$ (crosses in the upper right corner) or $G_{22}^2 = 0$ and $G_{11}^2 \neq 0$ (thin bullets), for fixed $\gamma = -3/4$ and $b = 1.5$ (black), $b = 1.2$ (green), $b = 0.9$ (red), $b = 0.8$ (blue), corresponding to the order from left to right in the lower half of the figure and opposite order in the upper part of the figure. Along the curves indicated by the dots (crosses) one has generically the $(\frac{5}{3}\text{L}, \text{KPZ})$ or $(\text{KPZ}, \frac{5}{3}\text{L})$ universality class. At the intersections of curves with the same colour one has the golden mean universality class $(\varphi\text{L}, \varphi\text{L})$.

In what follows we investigate in more detail the two novel universality classes $(\text{D}, \frac{3}{2}\text{L})$ and (GM, GM) which have not been reported yet in the literature on driven diffusive systems. We also comment on the shape of the structure function for the $\frac{5}{3}$ -mode discussed in [17].

IV. SUPERDIFFUSIVE NON-KPZ UNIVERSALITY CLASSES

A. Diffusive mode and 3/2-Lévy mode

We consider the case where mode 1 is Gaussian, and mode 2 has non-vanishing cross-coupling,

$$G_{11}^1 = G_{22}^1 = G_{22}^2 = 0, \quad G_{11}^2 \neq 0 \quad (36)$$

The mode coupling equation (17) for mode 2 reads in Fourier space

$$\partial_t \hat{S}_2(p, t) = -ipv_2 \hat{S}_2(p, t) - p^2 D_2 \hat{S}_2$$

$$-2(G_{11}^2)^2 p^2 \int_0^t ds \hat{S}_2(p, t-s) \int_{-\infty}^{\infty} dq \hat{S}_1((p-q, s) \hat{S}_1((q, s). \quad (37)$$

with $D_2 = \tilde{D}_{22}$. For the Gaussian mode 1 the mode coupling equation is obtained by the exchange $1 \leftrightarrow 2$ in (37) and dropping the term containing the integral. Note that we are interested in the large x behaviour of the scaling function, meaning $p \rightarrow 0$ in Fourier space.

We start with the observation that the Gaussian mode has the usual scaling form

$$S_1(x, t) = \frac{1}{\sqrt{4\pi D_1 t}} e^{-\frac{(x-v_1 t)^2}{4D_1 t}} \quad (38)$$

with Fourier transform $\hat{S}_1(p, t) = 1/\sqrt{2\pi} \exp(-iv_1 p t - D_1 p^2 t)$. Inserting this into (37) and performing the integration over q , we obtain

$$\partial_t \hat{S}_2(p, t) = -(ipv_2 + p^2 D_2) \hat{S}_2(p, t) - p^2 (G_{11}^2)^2 \int_0^t ds \hat{S}_2(p, t-s) \frac{e^{-iv_1 p s - D_2 p^2 s/2}}{\sqrt{2\pi D_2 s}}. \quad (39)$$

This equation can be solved in terms of the Laplace transform $\tilde{S}_2(p, \omega) := \int_0^\infty dt e^{-\omega t} \hat{S}_2(p, t)$ which yields

$$\tilde{S}_2(p, \omega) = \frac{\hat{S}_2(p, 0)}{\omega + ipv_2 + p^2 \left(D_2 + (G_{11}^2)^2 \left(\sqrt{2D_2(\omega + ipv_1 + D_2 p^2/2)} \right)^{-1} \right)}. \quad (40)$$

For large times we assume the real-space scaling form $S_2(x, t) = t^{-1/z} h\left(\frac{(x-v_2 t)^z}{t}\right)$ with dynamical exponent $z > 1$. This is equivalent to the scaling forms

$$\hat{S}_2(p, t) = e^{-iv_2 p t} f(|p|^z t), \quad \tilde{S}_2(p, \omega) = |p|^{-z} g\left(\frac{\omega + ipv_2}{|p|^z}\right) \quad (41)$$

for the Fourier- and Laplace transforms respectively. By introducing the shifted Laplace parameter $\tilde{\omega} := \omega + ipv_2$ one finds that the leading small- p behaviour of the Laplace transform (40) comes from the term proportional to $v_1 - v_2$ under the square root. This yields $z = 3/2$ and we obtain in the limit $\tilde{\omega} \rightarrow 0$ (with scaling variable $\tilde{\omega}/|p|^z$ kept fixed) after performing the inverse Laplace transformation

$$\hat{S}_2(p, t) = \frac{1}{\sqrt{2\pi}} \exp(-iv_2 p t - C_0 |p|^{3/2} t [1 - i \operatorname{sgn}(p(v_1 - v_2))]) \quad (42)$$

with

$$C_0 = \frac{(G_{11}^2)^2}{2\sqrt{D_1 |v_2 - v_1|}}. \quad (43)$$

We recognize here the characteristic function of an α -stable Lévy distribution

$$\hat{\phi}(p; \mu, c, \alpha, \beta) := \exp\left(ip\mu - |cp|^\alpha \left(1 - i\beta \tan\left(\frac{\pi\alpha}{2}\right) \text{sgn}(p)\right)\right) \quad (44)$$

with $\mu = -v_2 t$, $\alpha = 3/2$, $c = (C_0 t)^{2/3}$ and maximal asymmetry $\beta = \text{sgn}(v_1 - v_2) = \pm 1$.

We remark that in real space the asymmetric Lévy scaling function has only one heavy tail decaying as $1/x^{1+\alpha}$ which in a finite system leads to finite size corrections of order $1/L^{1+\alpha}$ for times $t \ll L^\alpha$. The other tail, that extends away from the position of the other mode, decays exponentially. This effect, which defines a kind of light cone, is a classical analogue of the Lieb-Robinson-bound for the spreading of perturbations in quantum systems [41]. The scaling function (42) is similar to the one found to describe the hydrodynamics of the anharmonic chain in the case of an "even potential", see [16].

Monte-Carlo simulation data for the 3/2-Lévy mode are shown in Fig. 4 for small times up to $t \approx 100$. The mode moves with a velocity that, numerically, cannot be distinguished from the theoretical prediction $v_2 = 1.3$. Indeed, one expects the error in the velocity, if at all, to be small, since the velocity comes from mass conservation and is an exact constant for all times even on the lattice [32].

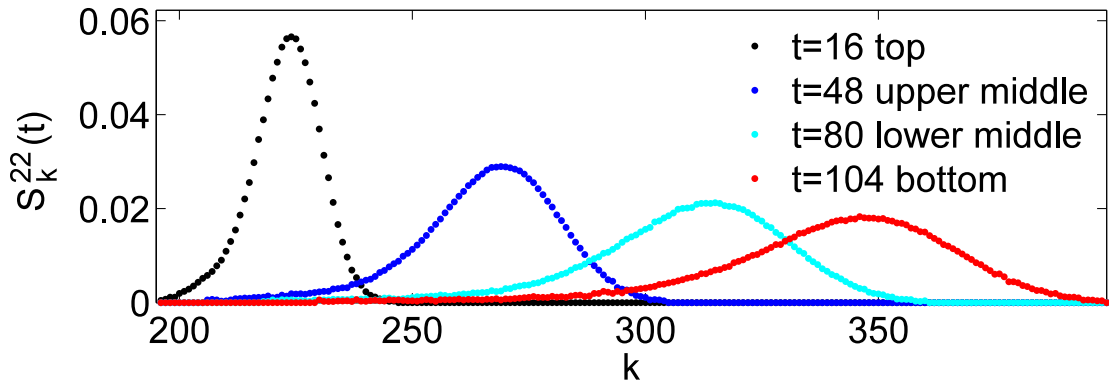


FIG. 4: (Colour online) Dynamical structure function $S_k^{22}(t)$ for 3/2-Lévy mode with $v_2 = 1.3$ measured by Monte Carlo simulation at different times, averaged over $18 \cdot 10^7$ histories. Parameters: $L = 600$, $\gamma = 2.5$, $b = 1$, $\rho_1 = 0.2$, $\rho_2 = 0.2$. Statistical errors are smaller than symbol size.

The scaling exponent and asymmetry predicted by mode coupling theory are in a good agreement with the Monte Carlo simulations, see Figs. 5, 6. In Fig. 5 we show the growth of the variance $V_2(t)$ of the measured 3/2-Lévy mode. This quantity is

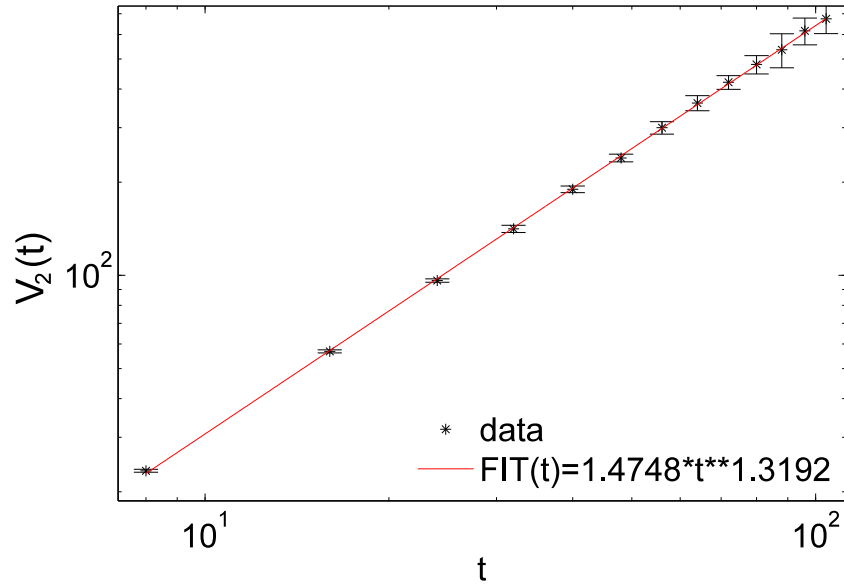


FIG. 5: (Color online) Variance $V_2(t)$ of the measured dynamical structure function shown in Fig. 4 versus time.

not infinite for finite times, since the (single) heavy tail of the asymptotic asymmetric Lévy scaling function (42) is cut off at finite times by the coupling to the other mode at a distance of the order $(v_2 - v_1)t$. Thus one expects the empirical variance $V_2(t)$ to be finite but growing in time. Mass conservation together with dynamical scaling predicts a growth $V_2(t) \propto t^\nu$ with $\nu = 2/z$ [17]. The measured exponent $\nu_{exp} \approx 1.32$ is very close to the theoretical value $\nu = 4/3$ even for the early time regime shown in the figures.

The only parameter that has slow convergence to the asymptotic value is the asymmetry of the scaling function. A similar phenomenon is discussed in [16] in terms of corrections to scaling of the memory kernel for the 5/3-Lévy mode. They are shown to vanish slowly with a power law decay in time. Here we measure the deviation of the asymmetry from its asymptotic value. The measured quantity $1 + \beta_{exp}$ decreases monotonically with time. The decay is approximately algebraic with exponent $\approx 1/6$, see Fig. 7.

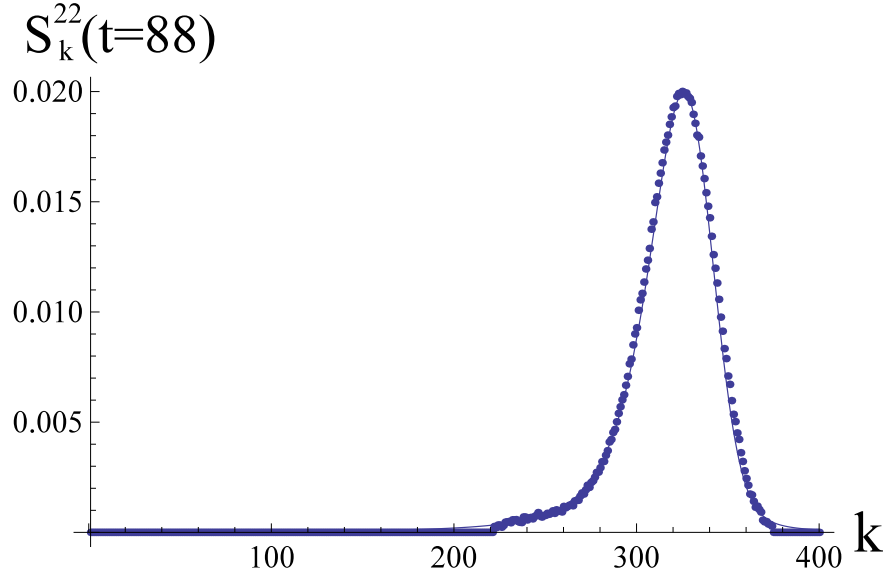


FIG. 6: (Colour online) Fit of the dynamical structure function $S_k^{22}(t)$ for time $t = 88$ with a 3/2-stable Lévy distribution with asymmetry $\beta = -0.692$. For parameters see Fig. 4.

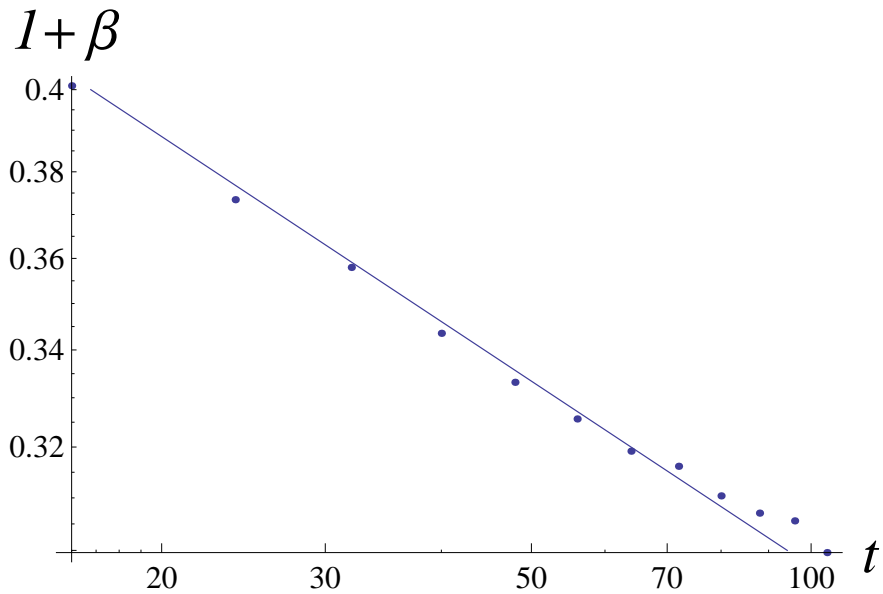


FIG. 7: (Colour online) Asymmetry $1 + \beta$ versus time, obtained by fitting the numerically obtained dynamical structure function with the PDF of 3/2 Lévy stable law. The line with the power law $\propto t^{-1/6}$ is a guide to the eye. For parameters see Fig. 4.

B. Two golden mean modes

We consider now the case where both self-coupling coefficients $G_{\alpha\alpha}^\alpha$ of the mode coupling matrix vanish and *both* subleading coefficients $G_{\beta\beta}^\alpha$ are non-zero and in general unequal. In this case one cannot use the Gaussian or the KPZ scaling function as an input into the mode coupling equations. However, the equations give a self-consistency relation which allows one to compute the scaling function for the two modes, see [39] for the symmetric case where $G_{22}^1 = G_{11}^2$. For the generic non-symmetric case $G_{22}^1 \neq G_{11}^2$ the calculation of [39] is not directly applicable. However, one can adopt a similar philosophy with two scaling functions

$$\hat{S}_1(p, t) = e^{-iv_1pt} g(b|p|t^\beta), \quad \hat{S}_2(p, t) = e^{-iv_2pt} h(c|p|^\gamma t) \quad (45)$$

as input, which, in addition to the *a priori* unknown dynamical exponents γ and $1/\beta$, have different scale factors b, c as free variables. With this ansatz one obtains by power counting the consistency conditions $\gamma = 1 + \beta$ and $\gamma = 1/\beta$ for the dynamical exponent. From the mode coupling equations we have computed also the scale factors. These computations are lengthy, but straightforward. With the relabelling $\hat{S}_-(p, t) \equiv \hat{S}_1(p, t)$, $\hat{S}_+(p, t) \equiv \hat{S}_2(p, t)$ one arrives at

$$\hat{S}_\pm(p, t) = \frac{1}{\sqrt{2\pi}} \exp\left(-iv_\pm pt - C_\pm |p|^\varphi t \left[1 \pm i \operatorname{sgn}(p(v_- - v_+)) \tan\left(\frac{\pi\varphi}{2}\right)\right]\right) \quad (46)$$

with golden mean $\gamma = \varphi \equiv (1 + \sqrt{5})/2$ and the scale factors

$$C_\pm = \frac{1}{2} |v_+ - v_-|^{1 - \frac{2}{\varphi}} \left(\frac{2G_{22}^1 G_{11}^2}{\varphi \sin\left(\frac{\pi\varphi}{2}\right)}\right)^{\varphi-1} \left(\frac{G_{22}^1}{G_{11}^2}\right)^{\pm(1+\varphi)}. \quad (47)$$

Notice that $\varphi - 1 = 1/\varphi$.

For numerical simulation of this new universality class we choose the parameter manifold (34) of the two-lane model where one has the characteristic velocities

$$v_\pm = (1 + \gamma\rho_2)(1 - 2\rho_1) \pm \gamma\sqrt{\rho_1(1 - \rho_1)\rho_2(1 - \rho_2)}. \quad (48)$$

We have chosen $\gamma = 2.5$, $b = 0.625$ and $\rho_1 = 0.25$, $\rho_2 = 0.2$ corresponding to the mode coupling matrices

$$G^1 = \begin{pmatrix} 0 & -0.406416 \\ -0.406416 & -0.105726 \end{pmatrix}, \quad G^2 = \begin{pmatrix} -0.812833 & -0.052863 \\ -0.052863 & 0 \end{pmatrix} \quad (49)$$

and transformation matrix

$$R^{-1} = \begin{pmatrix} -0.734553 & 0.734553 \\ 0.678551 & 0.678551 \end{pmatrix}. \quad (50)$$

The columns of R are the eigenmodes with velocities $v_1 \equiv v_- = 0.3170$, $v_2 \equiv v_+ = 1.183$ respectively. In order to measure the dynamical exponent $\varphi \approx 1.618$, which is rather close to $z = 5/3 \approx 1.667$ appearing in the (5/3L,KPZ) scenario studied in [17], we focus on the large-time regime rather than looking into corrections to scaling for the asymmetry as done above. We use simulation parameters $n = 300$, $m = 3$, $\tau = 120$ and $n = 1000$, $m = 46$, $\tau = 120$.

Fig. 8 shows the measured dynamical structure function for both golden modes moving on lattice 1. The peaks are well separated already at the earliest time $t = 480$ shown in the figure. The center of mass velocities have no perceptible deviation from the theoretical predictions.

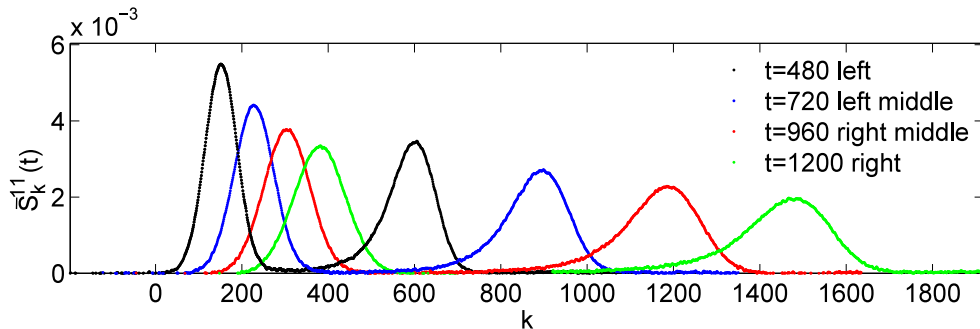


FIG. 8: (Colour online) Dynamical structure function showing both modes for particles on chain 1, for the golden mean mode with $v_2 = 1.183$ at different times. Parameters: $L = 10^6$, $\gamma = 2.5$, $b = 0.625$, $\rho_1 = 0.25$, $\rho_2 = 0.2$. Statistical errors are smaller than symbol size.

In Fig. 9 we plot the maximum of the dynamic structure function for mode 2 (which scale as $t^{-1/z}$) as a function of time. A least square fit with 95% confidence bounds gives a measured dynamical exponent $z = 1.619$, with error bars $1.613 < z < 1.624$. This agrees well with the theoretically predicted golden mean value $z = \varphi \approx 1.618$.

To investigate the convergence of the scaling function, we plot both the measured structure function and the theoretically predicted φ -stable distribution for a fixed time, see Fig. 10. The theoretical prediction is well borne out by the simulation. Small deviations

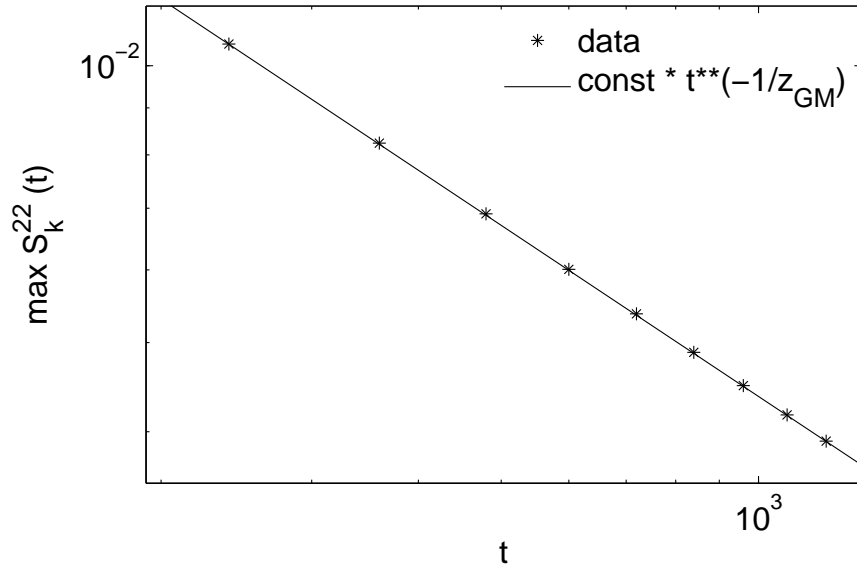


FIG. 9: (Color online) Maximum of the dynamical structure function for mode 2 versus time, plotted in double logarithmic scale. The line with the theoretically predicted slope (notice: $z_{GM} \equiv \varphi$) is a guide to the eye. Model parameters are as in Fig. 8.

are visible in the right (fast decaying) tail, see also the closeup view shown in the inset of Fig. 10. A fit with a maximally asymmetric 5/3-stable Lévy distribution shows a markedly poorer agreement.

Finally, we remark that the left peak in Fig. 8 corresponding to mode 1 is considerably less asymmetric than the peak of mode 2 shown in more detail in Fig. 10. To get some intuition for this observation we point out to the numerical values G_{22}^1 and G_{11}^2 (49). The ratio of their square is $(G_{22}^1/G_{11}^2)^2 \approx 0.017$, so the coupling strengths differ by almost two orders of magnitude. If G_{22}^1 was zero, we would be back to the $(D, \frac{3}{2}L)$ scenario discussed in the previous subsection and mode 1 would be a symmetric Gaussian peak. Therefore one indeed expects for mode 1 at finite times a more symmetric function than predicted for the asymptotic regime.

C. KPZ mode and 5/3-Lévy mode

In [17] we reported the occurrence of the $(\frac{5}{3}L, \text{KPZ})$ universality class for the totally asymmetric version of the two-lane exclusion process. The measured dynamical exponents

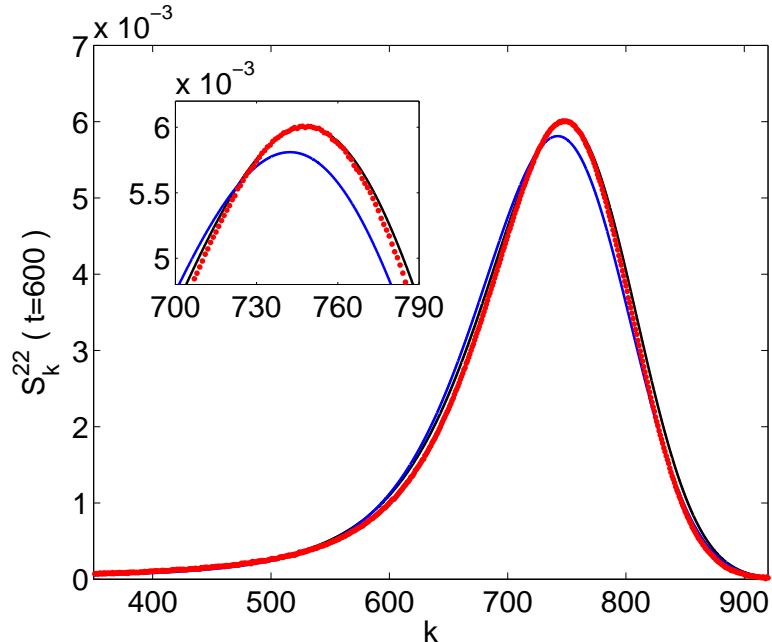


FIG. 10: (Color online) Measured dynamic structure function for mode 2 at time $t = 600$. Monte Carlo data correspond to red dots, and black (blue) curves correspond to the best least square fits of the Monte Carlo data with the $z = \varphi$ ($z = 5/3$) stable Lévy distribution with maximal asymmetry, and theoretically predicted center of mass position. The inset shows a close-up view of the peak region. Model parameters are as in Fig. 8.

were shown to agree well with the theoretical prediction. Here we expand on these result by briefly discussing the scaling function. In Fig. 11 one can see that a reasonable fit of the numerical data can be obtained with a $5/3$ -stable Lévy distribution predicted by mode coupling theory [16].

The measured dynamical structure function, however, exhibits an asymmetry much less than the predicted maximal value. Indeed, for small times its amplitude is rather small. We attribute this discrepancy to finite-time effects, cf. the argument for the left GM mode of the previous subsection. In order to substantiate this claim we show in Table II numerically determined asymmetries. They grow in time, thus supporting the argument. We do not have a theoretical prediction of how they should grow.

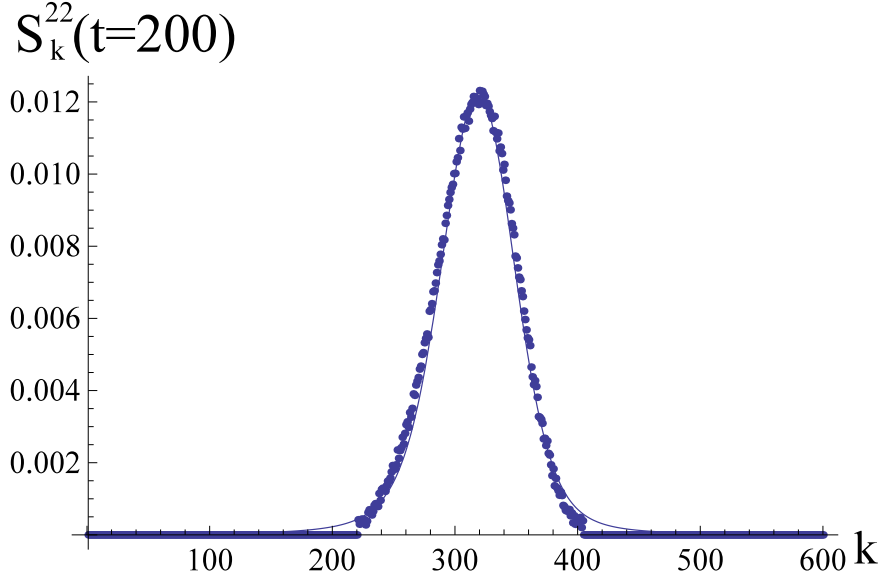


FIG. 11: (Color online) Measured dynamic structure function for mode 2 at time $t = 200$. The curve is a fit with the 5/3-stable Lévy distribution with non-maximal asymmetry..

t	20	40	60	80	100	120	140	160	200
β	-0.0229	-0.0504	-0.0685	-0.0797	-0.0825	-0.0872	-0.0918	-0.0916	-0.1000

TABLE II: Asymmetry β of a 5/3-Lévy distribution obtained from a fit to the numerical data for the 5/3-Lévy mode of [17] for different early times $t \leq 200$. The predicted asymptotic value is -1.

V. CONCLUSIONS

We have studied time-dependent density fluctuations in driven diffusive system with two conservation laws. For one conservation law it is well-established that the appropriate tool to describe the universal properties of these fluctuations is non-linear fluctuating hydrodynamics (9). Recent work, reviewed in [16], shows that the approach can be extended to anharmonic chains with more than one conservation law and also to Hamiltonian dynamics with three conservation laws [13]. From the present work and our preliminary results reported in [17] we conclude that the predictions of the theory apply also to driven diffusive systems with stochastic lattice gas dynamics with two conservation laws. Specifically, for a two-lane asymmetric simple exclusion process we argue that all theoretically possible universality classes for two-component systems, discussed also in [39], can be realized (see Table I). Among these, our Monte-Carlo simulations of a two-lane asymmetric exclusion

process confirm two superdiffusive universality classes which have gone unnoticed so far in the literature on driven diffusive systems.

Mode coupling theory not only predicts the dynamical exponents z for these universality classes, but also the scaling forms of the dynamical structure functions for these novel superdiffusive modes. In most cases these scaling functions are z -stable Lévy distributions with maximal asymmetry. The numerical simulation confirms these predictions with great accuracy both for the 3/2-mode and a golden mean mode with $z = (1 + \sqrt{5})/2$ shown to occur also in anharmonic chains [39]. For some modes the z -stable Lévy distributions provide excellent fits, but with an effective asymmetry that is not maximal. However, our data show that the numerically fitted asymmetry increases with time in the cases we considered, thus supporting the notion that asymptotically the maximal value will be reached.

Which universality classes actually occur in a system at given values of the physical parameters of the model is completely encoded in the stationary current-density relation $\vec{j}(\rho_1, \rho_2)$, no other knowledge about a given model is required. The stationary compressibility matrix $K(\rho_1, \rho_2)$, related to the current-density relation through a time-reversal symmetry proved in [36], allows for the prediction also of the scale factors that enter the scaling functions, unless diffusive modes are relevant. Thus generically the scaling functions are completely determined by two simple stationary properties: The current-density relation $\vec{j}(\rho_1, \rho_2)$ and the compressibility matrix $K(\rho_1, \rho_2)$. Going beyond specific lattice gas models, we have computed the mode coupling matrices in general form for arbitrary input data, i.e., arbitrary current-density relation and compressibility matrix. From the diagonal matrix elements of these one can then directly read off the scaling functions for arbitrary two-component systems, except in the presence of the diffusive universality class where the scale factors contain a phenomenological diffusion coefficient not predicted by the theory and which may modify the KPZ mode.

It is interesting to notice that all possible scenarios of universality classes (see Table I) can be realized with the simple current-density relation (2). This relation is minimal in the sense that the non-linearity of the conserved current j_λ is only quadratic and the coupling of this non-linearity to the other conserved quantity is only linear, i.e., $\rho_\lambda^2 \rho_\mu$ for $\lambda \neq \mu$. Thus it is not necessary to have a more complicated current-density relation in order to observe all allowed universality classes. Moreover, this minimal current-density relation has the nice property that one does not expect logarithmic corrections to diffusive modes [38].

Our two-lane exclusion process, which is an extension of the model studied by us previously [17], provides a simple microscopic realization for this minimal current-density relation.

Throughout this discussion we have tacitly assumed that the current-density relation is strictly hyperbolic, i.e., the collective velocities v_α of the two modes are different. This assumption is crucial for the decoupling argument for the modes that underlies the mode-coupling computations. Indeed, the nonequilibrium time reversal symmetry (A8) [36] rules out umbilic points (where $v_1 = v_2$) in any model which has minimal current-density relation and at the same time a diagonal compressibility matrix. Therefore in the model presented here the issue does not actually arise. However, umbilic points are a generic feature of more complicated models, either with the same minimal current-density relation, but a non-diagonal compressibility matrix [29], or for non-minimal current-density relations [40]. From numerical observations [40] one expects the dynamical exponent $z = 3/2$ as for KPZ, but non-KPZ scaling functions. How mode coupling theory can predict the behaviour at umbilic points is an open problem. It would also be interesting to extend mode coupling theory to predict the convergence of the finite-time asymmetry in the Lévy distribution to the asymptotic maximal value.

Acknowledgements

The authors are indebted to H. Spohn for pointing out the possibility of the golden mean universality class prior to publication of [39]. Indeed, this hint motivated us to systematically explore the structure of the mode-coupling matrices. We also thank him and G. Stoltz for useful comments on a preliminary version of the manuscript and M. Barma, R. Livi, H. Posch, A. Schadschneider and H. van Beijeren for enlightening discussions. Financial support by Deutsche Forschungsgemeinschaft (DFG) is gratefully acknowledged. We thank the INFN and the Galileo Galilei Institute for Theoretical Physics, where part of this work was done, for hospitality and for partial support.

Appendix A: Mode coupling matrices for strictly hyperbolic two-component systems

1. Notation

We consider a general system with two conservation laws. For definiteness we choose the language of driven diffusive systems with currents $j_\lambda(\rho_1, \rho_2)$, $\lambda = 1, 2$ for the conserved densities ρ_λ . We define the general flux Jacobian

$$J = \begin{pmatrix} J_{11} & J_{12} \\ J_{21} & J_{22} \end{pmatrix} \quad (\text{A1})$$

with matrix elements

$$J_{\lambda\mu} = \frac{\partial j_\lambda}{\partial \rho_\mu} \quad (\text{A2})$$

The transposed matrix is denoted J^T .

We define

$$\delta := (J_{11} - J_{22}) \sqrt{1 + \frac{4J_{12}J_{21}}{(J_{11} - J_{22})^2}} \quad (\text{A3})$$

which is the signed square root of the discriminant of the characteristic polynomial of J with the sign given by $J_{11} - J_{22}$. The two eigenvalues of J are

$$v_\pm = \frac{1}{2} (J_{11} + J_{22} \pm \delta). \quad (\text{A4})$$

We associate velocity v_- with eigenmode 1 and v_+ with eigenmode 2, irrespective of the sign of $v_- - v_+$ which is equal to the sign of $J_{22} - J_{11}$.

The matrix elements of the Hessians are denoted

$$H^\lambda = \begin{pmatrix} h_1^\lambda & \bar{h}^\lambda \\ \bar{h}^\lambda & h_2^\lambda \end{pmatrix} \quad (\text{A5})$$

with

$$h_1^\lambda = (\partial_1)^2 j_\lambda, \quad h_2^\lambda = (\partial_2)^2 j_\lambda, \quad \bar{h}^\lambda = \partial_1 \partial_2 j_\lambda. \quad (\text{A6})$$

They are symmetric by definition.

The compressibility matrix is denoted

$$K = \begin{pmatrix} \kappa_1 & \bar{\kappa} \\ \bar{\kappa} & \kappa_2 \end{pmatrix} \quad (\text{A7})$$

It is symmetric by definition. Without loss of generality we can assume $\kappa_1\kappa_2 \neq 0$ since a vanishing self-compressibility corresponds to a “frozen” lane without fluctuations which would reduce the dynamics of the two-lane system to a dynamics with a single conservation law. Time-reversal yields the Onsager-type symmetry [36]

$$JK = KJ^T \quad (\text{A8})$$

which implies

$$J_{21}\kappa_1 - J_{12}\kappa_2 = (J_{11} - J_{22})\bar{\kappa}. \quad (\text{A9})$$

Relation (A8) also guarantees that the eigenvalues v_{\pm} of a physical flux Jacobian J are generally real. A related symmetry relation was noted earlier in the context of classical fluids [34].

We point out the somewhat surprising fact that for *any* model with $\bar{\kappa} = 0$, i.e., whenever the stationary distribution factorizes in the conserved quantities, the compressibilities satisfy $J_{21}\kappa_1 = J_{12}\kappa_2$. Thus a vanishing cross derivative $J_{\lambda\mu}$ for one of the currents implies a vanishing cross derivative $J_{\mu\lambda}$ also of the other, without any *a priori* assumption on the stochastic dynamics. The same is true also on parameter manifolds where $J_{11} = J_{22}$.

2. Normal modes

We focus on the strictly hyperbolic case $v_+ \neq v_-$ corresponding to $\delta \neq 0$. Since J is not assumed to be symmetric we have to distinguish right (column) and left (row) eigenvectors, denoted by \bar{c}^{\pm} and \bar{r}^{\pm} , respectively. Here

$$\bar{c}^{\pm} = \begin{pmatrix} c_1^{\pm} \\ c_2^{\pm} \end{pmatrix}, \quad \bar{r}^{\pm} = (r_1^{\pm}, r_2^{\pm}). \quad (\text{A10})$$

We normalize them to obtain a biorthogonal basis with scalar product

$$\bar{r}^{\sigma} \cdot \bar{c}^{\sigma'} := r_1^{\sigma} c_1^{\sigma'} + r_2^{\sigma} c_2^{\sigma'} = \delta_{\sigma, \sigma'} \quad (\text{A11})$$

with $\sigma, \sigma' \in \{\pm\}$. Using

$$\frac{J_{22} - J_{11} - \delta}{2\sqrt{J_{12}J_{21}}} = \frac{2\sqrt{J_{12}J_{21}}}{J_{11} - J_{22} - \delta} \quad (\text{A12})$$

this yields

$$\bar{c}^{\pm} = \frac{1}{2\delta y_{\pm}} \begin{pmatrix} 2J_{12} \\ J_{22} - J_{11} \pm \delta \end{pmatrix}, \quad (\text{A13})$$

$$\vec{r}^\pm = \frac{y_\pm}{\delta \pm (J_{22} - J_{11})} (2J_{21}, J_{22} - J_{11} \pm \delta) \quad (\text{A14})$$

with arbitrary normalization constants y_\pm .

Next we introduce (bearing in mind that $\delta \neq 0$)

$$R = \begin{pmatrix} r_1^- & r_2^- \\ r_1^+ & r_2^+ \end{pmatrix}, \quad R^{-1} = \begin{pmatrix} c_1^- & c_1^+ \\ c_2^- & c_2^+ \end{pmatrix}. \quad (\text{A15})$$

Biorthogonality and normalization give $RR^{-1} = 1$. The fact that R contains the left eigenvectors as its rows implies $RJ = \Lambda R$ where $\Lambda = \text{diag}(v_-, v_+)$. Therefore

$$RJR^{-1} = \Lambda. \quad (\text{A16})$$

Then the linearized Eulerian hydrodynamic equations (7) read

$$\frac{\partial}{\partial t} \vec{\phi} + \Lambda \frac{\partial}{\partial x} \vec{\phi} = 0 \quad (\text{A17})$$

with $\vec{\phi} = R\vec{u}$.

The diagonalizer R is uniquely defined up to multiplication by an invertible diagonal matrix which is reflected in the arbitrariness of the normalization factors y_\pm . In order to fix these constants we first observe that from (A8) it follows that $R(JK)R^T = \Lambda(RKR^T) = R(KJ^T)R^T = (RKR^T)\Lambda$. Hence RKR^T must be diagonal since Λ is diagonal. This allows us to fix the normalization constants y_\pm by demanding

$$RKR^T = \mathbf{1}. \quad (\text{A18})$$

This normalization condition has its origin in the fact that the structure matrix $\bar{S}(k, t)$ (whose components are the dynamical structure functions (11)) is by definition normalized such that $\sum_k \bar{S}(k, t) = K$, see next subsection. For computing the normalization factors we first consider $J_{12}J_{21} \neq 0$.

It is convenient to parametrize R by diagonal matrices $Z = \text{diag}(z_-, z_+)$, $U = \text{diag}(1, u)$ and an orthogonal matrix O such that

$$R = ZOU = \begin{pmatrix} z_- \cos \vartheta & -uz_- \sin \vartheta \\ z_+ \sin \vartheta & uz_+ \cos \vartheta \end{pmatrix} \quad (\text{A19})$$

with

$$\tan \vartheta = \frac{J_{11} - J_{22} + \delta}{2\sqrt{J_{12}J_{21}}}, \quad u = \sqrt{\frac{J_{12}}{J_{21}}}. \quad (\text{A20})$$

Notice that $J_{12}J_{21} \neq 0$ implies $u \neq 0$, $\sin \vartheta \neq 0$ and $\cos \vartheta \neq 0$. There are several useful identities involving the rotation angle ϑ , viz. $\tan(2\vartheta) = 2\sqrt{J_{12}J_{21}}/(J_{22} - J_{11})$, $\sqrt{J_{12}J_{21}}(\cos^2 \vartheta - \sin^2 \vartheta) = (J_{22} - J_{11}) \cos \vartheta \sin \vartheta$ and $\delta = (J_{22} - J_{11})(\cos^2 \vartheta - \sin^2 \vartheta) + 4\sqrt{J_{12}J_{21}} \cos \vartheta \sin \vartheta = (J_{22} - J_{11}) \cos(2\vartheta) + 2\sqrt{J_{12}J_{21}} \sin 2\vartheta = (J_{22} - J_{11})/\cos(2\vartheta) = 2\sqrt{J_{12}J_{21}}/\sin(2\vartheta)$.

Now we use that for $\bar{\kappa} \neq 0$ one can write

$$UJU^{-1} = \mu UKU + \nu \mathbb{1} \quad (\text{A21})$$

with

$$\mu = \frac{J_{21}}{\bar{\kappa}}, \quad \nu = \frac{1}{2} \left(J_{11} + J_{22} - \frac{J_{21}\kappa_1 + J_{12}\kappa_2}{\bar{\kappa}} \right). \quad (\text{A22})$$

Therefore

$$\begin{aligned} RKR^T &= ZOUKUO^T Z = \frac{1}{\mu} (ZOUJU^{-1}O^T Z - \nu Z^2) \\ &= \frac{1}{\mu} \begin{pmatrix} v_- - z_-^2 \nu & 0 \\ 0 & v_+ - z_+^2 \nu \end{pmatrix} \end{aligned} \quad (\text{A23})$$

which yields

$$z_{\pm}^2 = \frac{v_{\pm} - \mu}{\nu}. \quad (\text{A24})$$

By comparing with (A15) one finds that the normalization factors for the eigenvectors are given by $y_- = uz_- \sin \vartheta$, $y_+ = uz_+ \cos \vartheta$. For $\bar{\kappa} = 0$ one obtains directly from (A9) and (A19) that

$$y_-^2 = \frac{\sin^2 \vartheta}{\kappa_2}, \quad y_+^2 = \frac{\cos^2 \vartheta}{\kappa_2}. \quad (\text{A25})$$

Even though not relevant for the two-lane model of this paper we mention for completeness that some care with limits has to be taken when $J_{12}J_{21} = 0$. First notice that in this case the physical requirement $\kappa_1\kappa_2 \neq 0$ implies $\bar{\kappa} \neq 0$. Specifically for $J_{12} = 0$, $J_{21} \neq 0$ one has $\delta = J_{11} - J_{22}$, $v_- = J_{11}$, $v_+ = J_{22}$, $J_{21}\kappa_1 = (J_{11} - J_{22})\bar{\kappa}$ and

$$R = \begin{pmatrix} \tilde{z}_- & 0 \\ \frac{\tilde{z}_+ J_{21}}{J_{22} - J_{11}} & \tilde{z}_+ \end{pmatrix} \quad (\text{A26})$$

with

$$\tilde{z}_-^{-2} = \kappa_1, \quad \tilde{z}_+^{-2} = \kappa_2 - \frac{\bar{\kappa}^2}{\kappa_1}. \quad (\text{A27})$$

Notice that here strict hyperbolicity implies $J_{11} \neq J_{22}$ so that R is well-defined.

Similarly one obtains for $J_{21} = 0$, $J_{12} \neq 0$ with $v_- = J_{11} \neq v_+ = J_{22}$ the relation $J_{12}\kappa_2 = (J_{22} - J_{11})\bar{\kappa}$ and

$$R = \begin{pmatrix} \hat{z}_- & \frac{\hat{z}_- J_{12}}{J_{11} - J_{22}} \\ 0 & \hat{z}_+ \end{pmatrix} \quad (\text{A28})$$

with

$$\hat{z}_-^{-2} = \kappa_1 - \frac{\bar{\kappa}^2}{\kappa_2}, \quad \hat{z}_+^{-2} = \kappa_2. \quad (\text{A29})$$

If $J_{12} = J_{21} = 0$ then J is diagonal. For the strictly hyperbolic case $J_{11} \neq J_{22}$ one necessarily has $\bar{\kappa} = 0$ and the normalization condition (A18) yields $R = \text{diag}(\kappa_1^{-1}, \kappa_2^{-1})$.

3. Normal modes and the microscopic dynamical structure function

In order to explain the origin of the normalization condition and to apply it to the two-lane model. We define the random variables $f_k^\lambda(t) := n_k^{(\lambda)}(t) - \rho_\lambda$ and $f_0^\lambda := f_0^\lambda(0)$ where the random variable $n_k^{(\lambda)}(t)$ is the particle number on site k of lane λ with particle density ρ_λ at time t . We also define the two-component column vector $\vec{f}_k(t)$ with components $f_k^\lambda(t)$ and the two-component row vector $\vec{f}_0^T := (f_0^1, f_0^2)$. Expectation w.r.t. the stationary distribution is denoted by $\langle \cdot \rangle$. By translation invariance and stationarity one has $\langle f_k^\lambda(t) \rangle = 0$. The expectation of a matrix is understood as the matrix of the expectations of its components. Defining the 2×2 -matrix $\vec{S}_k(t) = \vec{f}_k(t) \otimes \vec{f}_0^T$ (the components of which are random variables) the dynamical structure matrix with components (11) can be written $\bar{S}_k(t) = \langle \vec{S}_k(t) \rangle$.

The normalization of the dynamical structure matrix, defined by the sum over the whole lattice, is given by

$$\sum_k \bar{S}_k(t) = K. \quad (\text{A30})$$

It is independent of time because of translation invariance and particle number conservation. Now we consider the lattice normal modes

$$\vec{\phi}_k(t) = R \vec{f}_k(t) \quad (\text{A31})$$

with components $\phi_k^\alpha(t)$ where R is the diagonalizer (A15). In components

$$\phi_k^1(t) = r_{11} f_k^1(t) + r_{12} f_k^2(t), \quad \phi_k^2(t) = r_{21} f_k^1(t) + r_{22} f_k^2(t) \quad (\text{A32})$$

and similarly $\phi_0^\alpha := \phi_0^\alpha(0)$. In terms of the lattice normal modes the structure matrix has the form $S_k(t) := \langle \mathcal{S}_k(t) \rangle$ with $\mathcal{S}_k(t) := \vec{\phi}_k(t) \otimes \vec{\phi}_0^T$. This yields

$$S_k(t) = R\bar{S}_k(t)R^T \quad (\text{A33})$$

with matrix elements $S_{\alpha\beta}(k, t) = \langle \phi_k^\alpha(t)\phi_0^\beta \rangle$. The desired normalization

$$\sum_k S_k(t) = RKR^T = \mathbb{1} \quad (\text{A34})$$

leads to the requirement (A18).

4. Computation of the mode-coupling matrices

The mode-coupling coefficients are given by

$$G_{\alpha\beta}^\gamma := \frac{1}{2} \sum_\lambda R_{\gamma\lambda} [(R^{-1})^T H^\lambda R^{-1}]_{\alpha\beta}. \quad (\text{A35})$$

where $G_{\alpha\beta}^\gamma = G_{\beta\alpha}^\gamma$. Using the previous results one finds for G^1 the matrix elements

$$G_{11}^1 = \frac{1}{2z_-} [\cos^2 \vartheta (h_1^1 \cos \vartheta - uh_1^2 \sin \vartheta) + u^{-2} \sin^2 \vartheta (h_2^1 \cos \vartheta - uh_2^2 \sin \vartheta) - 2u^{-1} \cos \vartheta \sin \vartheta (\bar{h}^1 \cos \vartheta - u\bar{h}^2 \sin \vartheta)] \quad (\text{A36})$$

$$G_{22}^1 = \frac{z_-}{2z_+^2} [\sin^2 \vartheta (h_1^1 \cos \vartheta - uh_1^2 \sin \vartheta) + u^{-2} \cos^2 \vartheta (h_2^1 \cos \vartheta - uh_2^2 \sin \vartheta) + 2u^{-1} \cos \vartheta \sin \vartheta (\bar{h}^1 \cos \vartheta - u\bar{h}^2 \sin \vartheta)] \quad (\text{A37})$$

$$G_{12}^1 = \frac{1}{2z_+} [\cos \vartheta \sin \vartheta (h_1^1 \cos \vartheta - uh_1^2 \sin \vartheta - u^{-2} h_2^1 \cos \vartheta + u^{-1} h_2^2 \sin \vartheta) u^{-1} (\cos^2 \vartheta - \sin^2 \vartheta) (\bar{h}^1 \cos \vartheta - u\bar{h}^2 \sin \vartheta)], \quad (\text{A38})$$

and for G^2 one has

$$G_{22}^2 = \frac{1}{2z_+} [\sin^2 \vartheta (h_1^1 \sin \vartheta + uh_1^2 \cos \vartheta) + u^{-2} \cos^2 \vartheta (h_2^1 \sin \vartheta + uh_2^2 \cos \vartheta) + 2u^{-1} \cos \vartheta \sin \vartheta (\bar{h}^1 \sin \vartheta + u\bar{h}^2 \cos \vartheta)] \quad (\text{A39})$$

$$G_{11}^2 = \frac{z_+}{2z_-^2} [\cos^2 \vartheta (h_1^1 \sin \vartheta + uh_1^2 \cos \vartheta) + u^{-2} \sin^2 \vartheta (h_2^1 \sin \vartheta + h_2^2 u \cos \vartheta) - 2u^{-1} \cos \vartheta \sin \vartheta (\bar{h}^1 \sin \vartheta + u\bar{h}^2 \cos \vartheta)] \quad (\text{A40})$$

$$G_{12}^2 = \frac{1}{2z_-} [\cos \vartheta \sin \vartheta (h_1^1 \sin \vartheta + uh_1^2 \cos \vartheta - u^{-2} h_2^1 \sin \vartheta - u^{-1} h_2^2 \cos \vartheta) u^{-1} (\cos^2 \vartheta - \sin^2 \vartheta) (\bar{h}^1 \sin \vartheta + u\bar{h}^2 \cos \vartheta)]. \quad (\text{A41})$$

In terms of the model parameters $a, b, c, d, \kappa_{1,2}, \bar{\kappa}$ The quantities ϑ and u are given in (A20) and the quantities z_{\pm} are given in (A24). The parameter δ appearing in (A20) is given in (A3).

In order to analyze the manifolds where diagonal elements of the mode coupling matrices vanish it is convenient to introduce

$$g_1^1 := h_1^1, g_2^1 := u^{-2}h_2^1, \bar{g}^1 := u^{-1}\bar{h}^1 \quad (\text{A42})$$

$$g_1^2 := uh_1^2, g_2^2 := u^{-1}h_2^2, \bar{g}^2 := \bar{h}^2. \quad (\text{A43})$$

and define the polynomials

$$D_1^1(\omega) := g_1^1 - (g_1^2 + 2\bar{g}^1)\omega + (g_2^1 + 2\bar{g}^2)\omega^2 - g_2^2\omega^3 \quad (\text{A44})$$

$$D_2^1(\omega) := g_2^1 - (g_2^2 - 2\bar{g}^1)\omega + (g_1^1 - 2\bar{g}^2)\omega^2 - g_1^2\omega^3 \quad (\text{A45})$$

$$D_1^2(\omega) := g_1^2 + (g_1^1 - 2\bar{g}^2)\omega + (g_2^2 - 2\bar{g}^1)\omega^2 + g_2^1\omega^3 \quad (\text{A46})$$

$$D_2^2(\omega) := g_2^2 + (g_2^1 + 2\bar{g}^2)\omega + (g_1^2 + 2\bar{g}^1)\omega^2 + g_1^1\omega^3. \quad (\text{A47})$$

with $\omega := \tan \vartheta$. Only the Hessian and the parameters u and $\tan \vartheta$ given in (A20) enter these functions. They do not depend on the compressibilities. Then one has

$$G_{11}^1 = \frac{\cos^3 \vartheta}{2z_-} D_1^1(\omega), \quad G_{22}^1 = \frac{z_- \cos^3 \vartheta}{2z_+^2} D_2^1(\omega) \quad (\text{A48})$$

$$G_{11}^2 = \frac{z_+ \cos^3 \vartheta}{2z_-^2} D_1^2(\omega), \quad G_{22}^2 = \frac{\cos^3 \vartheta}{2z_+} D_2^2(\omega). \quad (\text{A49})$$

Notice the symmetry properties $D_1^1(\omega) = -\omega^3 D_2^2(-\omega^{-1})$ and $D_2^1(\omega) = -\omega^3 D_1^2(-\omega^{-1})$.

-
- [1] S. Lepri, R. Livi, A. Politi, Thermal conduction in in classical low-dimensional lattices. Phys. Rep. **377**, 1–80 (2003).
 - [2] M. Kardar, G. Parisi, and Y.-C. Zhang, Dynamic scaling of growing interfaces. Phys. Rev. Lett. **56**, 889–892 (1986).
 - [3] M. Prähofer and H. Spohn, Exact scaling functions for one-dimensional stationary KPZ growth. J. Stat. Phys. **115**, 255–279 (2004).
 - [4] M. Prähofer and H. Spohn, in: *In and Out of Equilibrium*, edited by V. Sidoravicius, Vol. 51 of Progress in Probability (Birkhauser, Boston, 2002).

- [5] L. Miettinen, M. Myllys, J. Merikoski, and J. Timonen, Experimental determination of KPZ height-fluctuation distributions. *Eur. Phys. J. B* **46**, 55–60 (2005).
- [6] K.A. Takeuchi and M. Sano, Universal fluctuations of growing interfaces: evidence in turbulent liquid crystals. *Phys. Rev. Lett.* **104**, 230601 (2010).
- [7] P.F. Arndt, T. Heinzl, and V. Rittenberg, Spontaneous breaking of translational invariance in one-dimensional stationary states on a ring. *J. Phys. A: Math. Gen.* **31** L45–L51 (1998)
- [8] P.L. Ferrari, T. Sasamoto and H. Spohn, Coupled Kardar-Parisi-Zhang equations in one dimension. *J. Stat. Phys.* **153**, 377–399 (2013).
- [9] D. Huse, B. Kaufmann and G.M. Schütz, work in progress.
- [10] A. Rákos and G.M. Schütz, Exact shock measures and steady state selection in a driven diffusive system with two conserved densities. *J. Stat. Phys.* **117**, 55–76 (2004).
- [11] D. Das, A. Basu, M. Barma, and S. Ramaswamy, Weak and strong dynamic scaling in a one-dimensional driven coupled-field model: Effects of kinematic waves. *Phys. Rev. E* **64**, 021402 (2001).
- [12] A. Nagar, M. Barma, and S. N. Majumdar, Passive Sliders on Fluctuating Surfaces: Strong-Clustering States. *Phys. Rev. Lett.* **94**, 240601 (2005).
- [13] H. van Beijeren, Exact results for anomalous transport in one-dimensional Hamiltonian systems. *Phys. Rev. Lett.* **108**, 108601 (2012).
- [14] C.B. Mendl and H. Spohn, Dynamic correlators of FPU chains and nonlinear fluctuating hydrodynamics. *Phys. Rev. Lett.* **111**, 230601 (2013).
- [15] S. G. Das, A. Dhar, K. Saito, Ch. B. Mendl, and H. Spohn, Numerical test of hydrodynamic fluctuation theory in the Fermi-Pasta-Ulam chain. *Phys. Rev. E* **90**, 012124 (2014)
- [16] H. Spohn, Nonlinear Fluctuating hydrodynamics for anharmonic chains. *J. Stat. Phys.* **154**, 1191–1227 (2014).
- [17] V. Popkov, J. Schmidt, and G.M. Schütz, Superdiffusive modes in two-species driven diffusive systems. *Phys. Rev. Lett.* **112**, 200602 (2014).
- [18] C. Bernardin and P. Gonçalves, Anomalous fluctuations for a perturbed Hamiltonian system with exponential interactions. *Commun. Math. Phys.* **325**, 291–332 (2014).
- [19] M. R. Evans, D. P. Foster, C. Godrèche, and D. Mukamel, Symmetric Exclusion Model with Two Species: Spontaneous Symmetry Breaking. *Phys. Rev. Lett.* **74**, 208–211 (1995).
- [20] V. Popkov and I. Peschel, Symmetry breaking and phase coexistence in a driven diffusive

- two-channel system. *Phys. Rev. E* **64** 026126 (2001).
- [21] R.D. Willmann, G.M. Schütz, and S. Großkinsky, Dynamical origin of spontaneous symmetry breaking in a field-driven nonequilibrium system. *Europhys. Lett.* **71** 542–547 (2005).
- [22] V. Popkov, M. R. Evans, and D. Mukamel, Spontaneous symmetry breaking in a bridge model fed by junctions. *J. Phys. A* **41**, 432002 (2008).
- [23] S. Gupta, D. Mukamel, and G.M. Schütz, Robustness of spontaneous symmetry breaking in a bridge model. *J. Phys. A: Math. Theor.* **42**, 485002 (2009)
- [24] M.R. Evans, Y. Kafri, H.M. Koduvely, and D. Mukamel, Phase separation and coarsening in one-dimensional driven diffusive systems: Local dynamics leading to long-range Hamiltonians. *Phys. Rev. E* **58** 2764–2778 (1998).
- [25] R. Lahiri, M. Barma, and S. Ramaswamy, Strong phase separation in a model of sedimenting lattices. *Phys. Rev. E* **61**, 1648–1658 (2000).
- [26] J.T. Mettetal, B. Schmittmann, and R.K.P. Zia , Coarsening dynamics of a quasi-one-dimensional driven lattice gas. *Europhys. Lett.* **58**, 653–658 (2002).
- [27] M. Clincy and M.R. Evans, Phase transition in the ABC model. *Phys. Rev. E* **67** 066115 (2003).
- [28] G.M. Schütz, Critical phenomena and universal dynamics in one-dimensional driven diffusive systems with two species of particles. *J. Phys. A: Math. Gen.* **36**, R339–R379 (2003).
- [29] V. Popkov and G.M. Schütz, Unusual shock wave in two-species driven systems with an umbilic point. *Phys. Rev. E* **67** 031139 (2012).
- [30] V. Popkov, *Eur. Phys. J. Special Topics* **216**, 139–151 (2013)
- [31] G.M. Schütz, R. Ramaswamy and M. Barma, Pairwise balance and invariant measures for generalized exclusion processes, *J. Phys. A: Math. Gen.* **29**, 837–845 (1996).
- [32] V. Popkov and G.M. Schütz, Shocks and excitation dynamics in a driven diffusive two-channel system, *J. Stat. Phys.* **112**, 523–540 (2003).
- [33] V. Popkov and M. Salerno, Hydrodynamic limit of multichain driven diffusive models. *Phys. Rev. E* **69**, 046103 (2004).
- [34] H. Spohn, *Large Scale Dynamics of Interacting Particles*. (Springer, Berlin, 1991)
- [35] C. Kipnis and C. Landim, *Scaling limits of interacting particle systems* (Springer, Berlin, 1999)
- [36] R. Grisi and G.M. Schütz, Current symmetries for particle systems with several conservation laws. *J. Stat. Phys.* **145**, 1499–1512 (2011).

- [37] B. Tóth and B. Valkó, *J. Stat. Phys.* **112**, 497–521 (2003).
- [38] P. Devillard and H. Spohn, Universality class of interface growth with reflection symmetry. *J. Stat. Phys.* **66**, 1089–1099 (1992).
- [39] H. Spohn and G. Stoltz, Nonlinear fluctuating hydrodynamics in one dimension: The case of two conserved fields. to appear in *J. Stat. Phys.*, same volume (2015).
- [40] D. Ertas and M. Kardar, Dynamic roughening of directed lines. *Phys. Rev. Lett.* **69**, 929–932 (1992).
- [41] E. Lieb, D. Robinson, The finite group velocity of quantum spin systems. *Commun. Math. Phys.* **28**, 251-257, (1972)
- [42] We choose the same notation as for the empirical structure function obtained from Monte-Carlo simulations presented below.